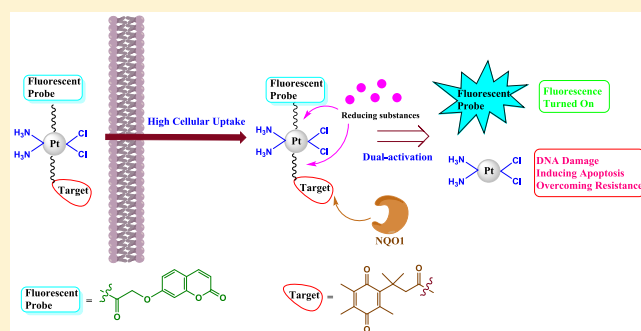


Construction of Dual Stimuli-Responsive Platinum(IV) Hybrids with NQO1 Targeting Ability and Overcoming Cisplatin Resistance

Lei Fang,^{†,‡} Xiaodong Qin,[†] Jian Zhao,[†] and Shaohua Gou^{*,†} [†]Jiangsu Province Hi-Tech Key Laboratory for Bio-Medical Research, School of Chemistry and Chemical Engineering, Southeast University, Nanjing 211189, China[‡]State Key Laboratory for Chemistry and Molecular Engineering of Medicinal Resources, Guangxi Normal University, Guilin 541004, China Supporting Information

ABSTRACT: Quinone oxidoreductase isozyme I (NQO1) is a cytoprotective two-electron-specific reductase that highly expresses in various cancer cells. Taking NQO1 as the target, we herein report three hybrid compounds from Pt(IV) complexes and a quinone propionic acid unit. The mechanism studies showed that the hybrids could be activated by both NQO1 and ascorbic acid to release the cytotoxic Pt(II) unit, exhibiting a dual stimuli-responsive character. In the pharmacological studies, complexes 2 and 3 presented higher antitumor activity than cisplatin. More importantly, the hybrid could also overcome cisplatin resistance due to the NQO1 targeting ability, improved cellular uptake, and/or different action mechanism. Significantly, complex 3 containing a coumarin moiety could be effectively activated in NQO1-overexpressed cancer cells to “turn on” fluorescence, showing a promising visual effect in cancer cells. In vivo study revealed that both 2 and 3 exhibited higher antitumor efficacy than cisplatin in the A549 xenograft mouse model at an equimolar dose to cisplatin. In all, the hybrids may serve as promising NQO1-targeting anticancer agents.



■ INTRODUCTION

To date, lung cancer has been becoming one of the most leading causes of cancer deaths in the world.¹ In spite of outstanding advances made in the treatment of lung cancer over the last decades, the clinical treatment is still unsatisfactory. For example, chemotherapy is the main “weapon” for the patients to fight lung cancer, but it is often limited by high toxicity, nonspecificity, and drug resistance.^{2,3} In a quest to improve the therapeutic efficiency, a large variety of novel antitumor therapies have emerged, among which the tumor-targeting agents attract the most attention since they can selectively kill the tumor cells and induce slight toxic effects on healthy tissues. Usually the tumor targeting ability is obtained by the specific response to the unique tumor microenvironments, such as high glutathione and reactive oxygen species (ROS) levels, cellular receptors, low pH values as well as overexpressed enzymes.^{4–9} NAD(P)H oxidoreductase (quinone)-1 (NQO1, also known as DT-diaphorase) has been found widely present in many human tumors (e.g., lung, colon, breast, liver, and ovary tumors), and the levels are 2- to 50-fold higher than those in normal tissues.^{10,11} Recently many studies found NQO1 may be an indicator of prognosis in lung cancer, especially in nonsmall cell lung cancer (NSCLC).¹² Indeed NQO1 is intimately involved in cancer since it plays an important role in the 20S proteasomal degradation of p53, p73 α , and p33 tumor suppressors. Some cytotoxic quinone

drugs that act on the NQO1 pathway have shown excellent anticancer activity, indicating NQO1 is a valid target for tumor treatment.^{13,14} Apart from being the action target, NQO1 can also be employed as a trigger to activate fluorescent probes or quinone prodrugs. For example, McCarley et al. used a quinone propionic acid moiety as the trigger group to create self-immolative profluorophores which could effectively be degraded by NQO1 to release fluorescent probes.¹⁵ These findings suggest that design of NQO1-responsive compounds may be a promising strategy to find targeting antitumor agents.

Cisplatin (CDDP) is one of the most used chemotherapeutic agents for the treatment of lung cancer,¹⁶ however, its nonspecific toxicity to both tumor and healthy tissues causes severe side effects.¹⁷ In order to overcome these drawbacks, Pt(IV) complexes acting as prodrugs of their Pt(II) counterparts have emerged, because they can release active Pt(II) species upon reduction by cellular biomolecular agents such as glutathione and ascorbic acid (VC). As compared with Pt(II) complexes, Pt(IV) complexes can offer two valuable axial positions to which many interesting structural modifications can be made, resulting in various hybrid compounds. Such Pt(IV) hybrid compounds like Asplatin, NERi-Pt(IV), and Chalcoplatin showed remarkable antitumor activity due to the

Received: December 4, 2018

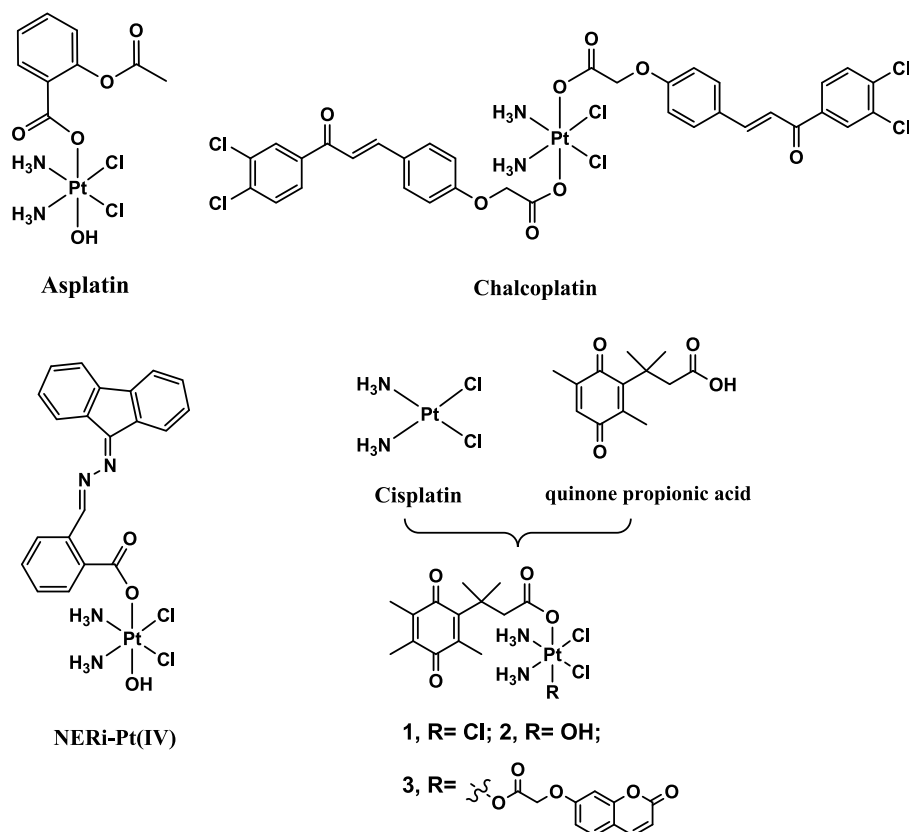


Figure 1. Chemical structures of cisplatin, several known Pt(IV) complexes and the designed platinum(IV) hybrids.

introduction of the bioactive moiety to the axial position (Figure 1).^{18–24} The current progresses concerning the Pt(IV) prodrugs have been well reviewed by Lippard and Gibson.^{25,26} However, these prodrugs still lack tumor-targeting ability.

To take advantage of the NQO1 as the target, we have designed three NQO1-activatable Pt(IV) complexes by linking a quinone propionic acid moiety to the axial position of the metal atom (Figure 1). In this design, the quinone propionic acid was supposed to act as a targeted group because these Pt(IV) complexes can be rapidly and selectively reduced to the Pt(II) counterpart by tumor cells in which NQO1 is overexpressed.^{14,15} Furthermore, a fluorescent coumarin moiety (11) was attached to the other axial position in Pt(IV) complex 3 to observe its behavior in cancer cells. We hypothesized that this kind of Pt(IV) prodrug could function as a dual stimuli-responsive prodrug to both NQO1 and other biomolecular agents like VC.

RESULTS AND DISCUSSION

Synthesis and Characterization. As depicted in Scheme 1, quinone propionic acid was first synthesized according to a known procedure,²⁷ and Pt(IV) intermediates 7 and 8 were prepared as described previously.²⁸ Interaction of quinone propionic acid with two Pt(IV) intermediates, respectively, was then made in the presence of *O*-(benzotriazol-1-yl)-*N,N,N',N'*-tetramethyluronium tetrafluoroborate (TBTU) to yield complexes 1 and 2. Complex 3 was obtained by further reaction of 2 with a coumarin derivative. All the resulting compounds were characterized by microanalyses, ¹H, ¹³C, and ¹⁹⁵Pt NMR spectroscopy together with ESI-HRMS spectrometry.

Stability and Reduction Potential of Hybrid Compounds. In our drug design strategy, the hybrid compounds

should be stable under normal physiological condition while could release bioactive units upon cellular reducing substances such as VC. Thereby, the stability of 1–3 under different pH values in phosphate buffer saline (PBS) was examined by using UV/vis absorption spectrophotometry, respectively (Figures S1–S3). For complex 1 in PBS (pH = 7.4), the 267 nm absorption peak decreased slightly after 24 and 48 h incubation (ca. 90% of 1 remained intact over 48 h), which meant small amounts of hydrolysis occurred. Under the weak acidic condition (pH = 6.5 or 5.6), the decrease of absorbance accelerated, indicating that acidity influenced the hydrolysis of 1. As for complex 2, ca. 95% of the complex remained intact over 48 h. In contrast, no apparent hydrolysis of 3 occurred in different PBS. The result indicated that 1 was the least stable complex, while 3 was the most stable one. The stability of 1–3 in biological media was also evaluated by HPLC. The retention time of the medium and the FBS was ca. 3 min, while the retention time of the tested compounds was in the range from 6 to 10 min. As shown in Figures 2A and S4, after 24 h incubation in medium RPMI-1640 containing 10% FBS, ca. 98% of 3, 96% of 2, and 92% of 1 remained unchanged, indicating good stability of the complexes under the test condition.

As the stability of 1–3 was confirmed, we further investigated the reduction potential of 1–3 and 6–8 using cyclic voltammetry (CV) (Figure S5). All the complexes displayed irreversible reduction processes with several different peak potentials (Figure S5). Complex 1 containing a Cl ligand at the axial position showed a peak potential at ca. –400 mV, which was similar to the value reported by Bellemin-Lapponaz et al.²⁹ In contrast, complexes 2 and 3 which contained OH or the ester ligand at the axial position showed peak potential at ca.

Scheme 1. Synthesis of NQO1-Targeted Pt(IV) Complexes 1–3

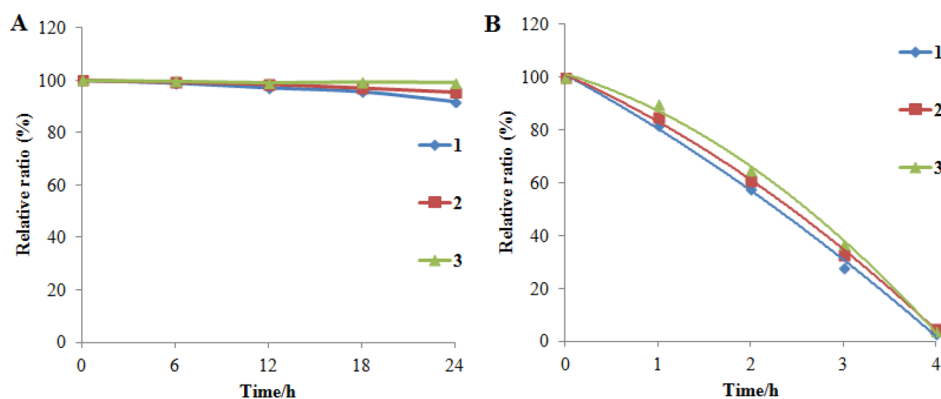
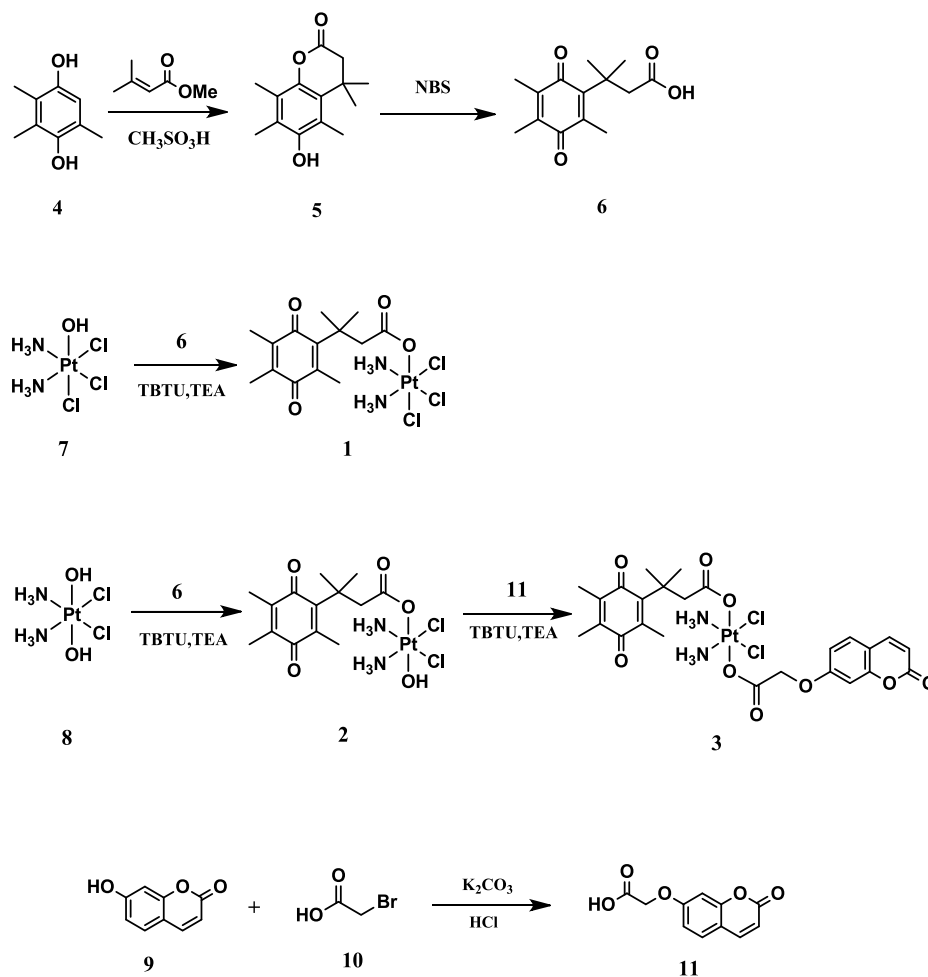


Figure 2. (A) The stability of prodrugs 1–3 (0.1 mM, 37 °C) in medium RPMI-1640. (B) Time-dependent responses of prodrugs 1–3 to NQO1 in the presence of the cofactor NADH; prodrugs 1–3 were dissolved in PBS containing 5% DMF at the concentration of 0.1 mM (37 °C).

–700 mV. The lower peak potential of 1 suggested the easier reduction of the complex, which was consistent with the results of the stability study. As compared complexes 7 and 8, the peak potentials of 2 and 3 were significantly enhanced from ca. –300 mV to ca. –700 mV, indicating the conversion of OH to the ester form improved the stability. Among all of the complexes, the chemical reduction of complex 2 with an axial hydroxyl was more difficult than complex 1 with an axial chloridion, indicating that the chloridion ligand could promote the transfer of electrons better than the hydroxyl ligand. The

reduction of 3 is most difficult, demonstrating that the carboxylate somehow hindered the transfer of electrons from the reducing agent to the Pt(IV) center in comparison to the chloridion and hydroxyl group.

In Vitro Cytotoxicity. With the good performance of 1–3 in the tests of stability and reduction potential, the cytotoxicity of 1–3 was evaluated against A549 and A549/CDDP cells in high levels of NQO1 as well as HepG2 and LO2 cells in low levels of NQO1 (Table 1).^{30,31} As anticipated, cisplatin displayed cytotoxic effects on all tested cells indiscriminate of

Table 1. In Vitro Cytotoxicity of Cisplatin, 6, 11, and 1–3

compd	IC ₅₀ (μM)				RF ^a
	LO2(NQO1-)	HepG2(NQO1-)	A549(NQO1+)	A549/CDDP(NQO1+)	
cisplatin	13.02 ± 1.26	6.71 ± 0.47	5.37 ± 0.11	28.44 ± 1.17	5.3
6	>100	>100	>100	>100	—
11	>100	>100	>100	>100	—
1	16.39 ± 1.36	7.37 ± 0.38	6.72 ± 0.21	31.20 ± 1.26	4.6
2	10.33 ± 1.35	8.26 ± 0.85	0.49 ± 0.02	0.79 ± 0.15	1.6
3	8.29 ± 1.07	3.06 ± 0.34	1.05 ± 0.14	1.94 ± 0.21	1.8

^aResistance factor, IC₅₀(A549/CDDP)/IC₅₀ (A549). The data represent the mean values of at least three independent experiments.

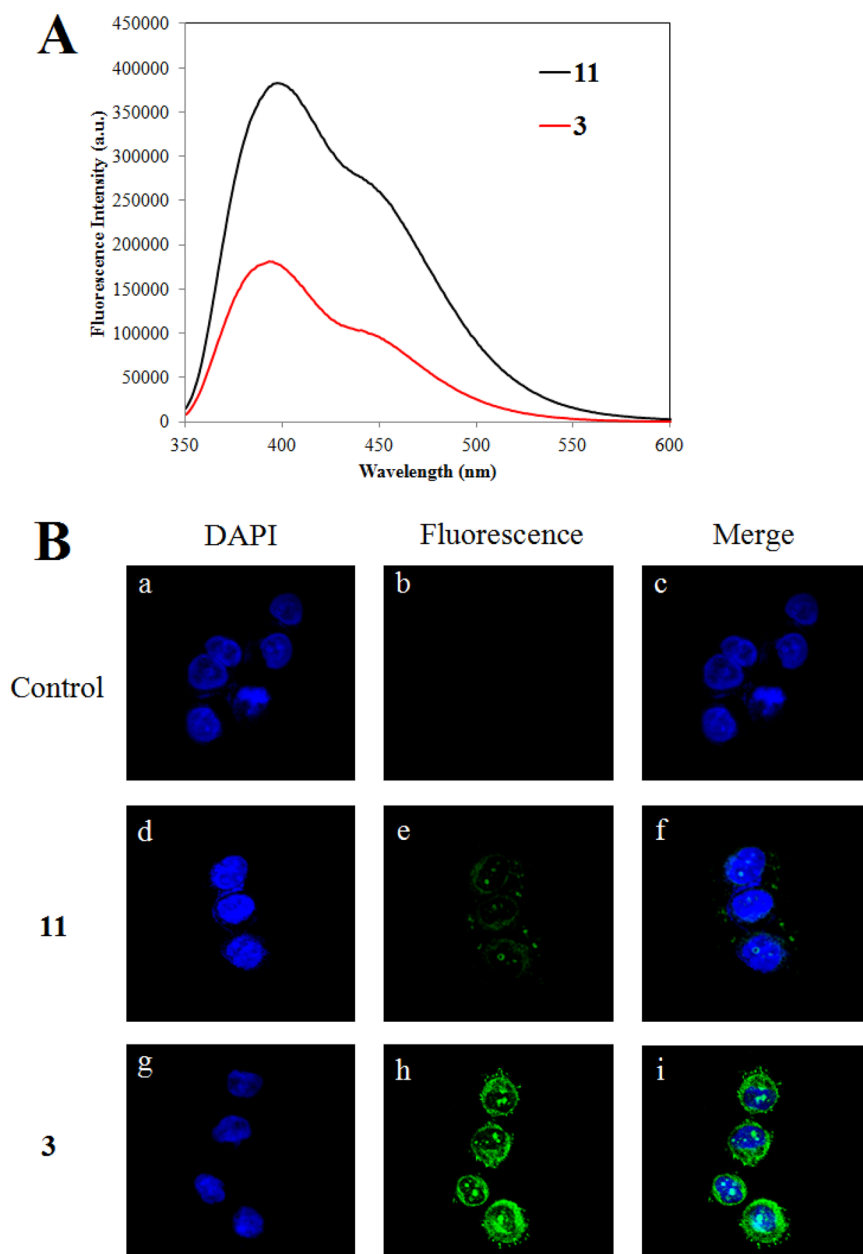


Figure 3. (A) Fluorescence spectra of 11 and 3. The tested compounds were dissolved in PBS containing 5% DMF and the final concentration was 10 μM (37 °C). (B) Confocal microscopy pictures of A549 (NQO1+) cells when treated with 11 (d–f), 3 (g–i), or blank control cells (a–c) for 3 h.

NQO1 levels. The IC₅₀ values of 1 were between 6.72 μM and 31.20 μM, comparable to cisplatin but much weaker than 2 and 3 toward the cells in a high expression of NQO1. This might be attributed to the fast reducibility of 1, which led to

undesired degradation in extracellular environment. Although displaying a micromolar level of IC₅₀ values, 1–3 did not show apparent enhanced cytotoxicity against HepG2 cells compared to cisplatin. Significantly, the IC₅₀ values of 2 and 3 were 11-

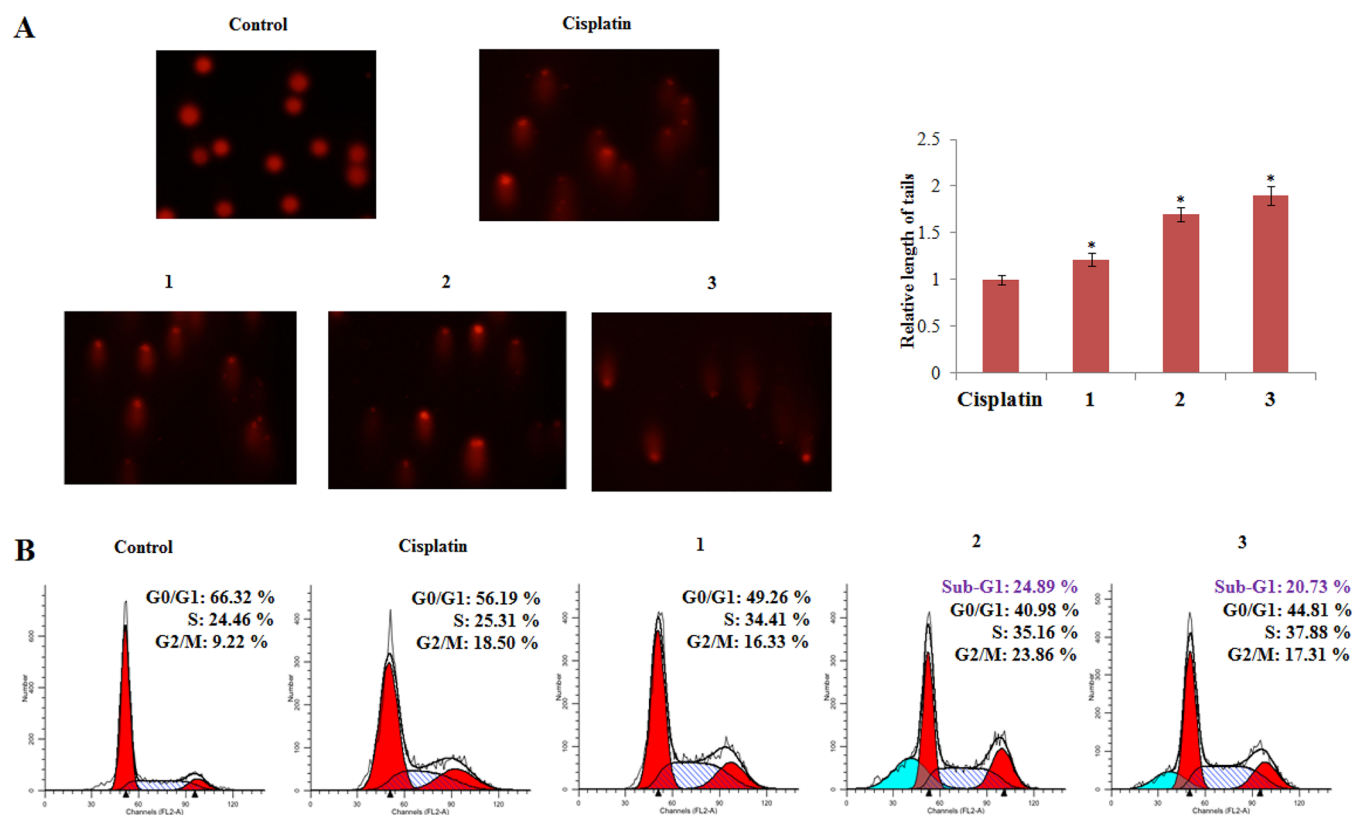


Figure 4. (A) Analysis of the relative length of DNA tails in the comet assay. * $P < 0.05$, compared with cisplatin group. (B) Cell cycle distribution of A549 cells when treated with cisplatin or complexes 1–3 at $5 \mu\text{M}$ for 24 h.

fold and 5-fold lower than cisplatin in A549 cells, respectively. Particularly noteworthy are the results obtained toward A549/CDDP cells. Both 2 and 3 displayed strong ability to overcome drug resistance in comparison with cisplatin. In addition, the cytotoxicity of 2 and 3 in LO2 normal cells was remarkably lower than that in A549 cells, further verifying the selectivity of 2 and 3 toward NQO1+ cells.

Responsive Property of Complexes 1–3. In order to further confirm the targeting property of the complexes, NQO1 and VC dual stimuli-responsive tests were performed. When treated with NQO1 and the cofactor NADH, all three complexes could be decomposed as the time passed (Figure 2B). The decomposition proceeded very fast. All three complexes disappeared within 4 h under the test conditions. Notably, the decomposition rate of 1–3 was basically similar, demonstrating that NQO1-triggered activation was independent of the coordination structure of the Pt(IV) complexes. When treated with VC, complex 1 was effectively reduced by VC and simultaneously released compound 6 as reflected by the increasing peak of 6 in a time-dependent manner (Figures S6–S8). As for 2 and 3, the reduction could also be observed when incubated with VC. It was noticed that the reduction caused by VC seemed slower than NQO1, as the tested complexes could be observed even after 9 h or longer co-incubation with ascorbate. The experimental data of complexes 1–3 fit well to a monoexponential function, and the so-obtained constants (k_{obs}) were 0.2399 h^{-1} , 0.0576 h^{-1} , and 0.0273 h^{-1} , respectively. Obviously, complex 1 with an axial chlorido group exhibited the fastest reduction rate, which is 4.2-fold and 8.8-fold faster than complexes 2 and 3, respectively (Figure S9). This is probably because chloridic ligands are apt to form a bridge with ascorbate,³² which may

promote the transfer of electrons from ascorbate to the metal center. Moreover, complex 2 with one hydroxido ligand is easier to form a bridge with the reducing agents than complex 3 with two carboxylato ligands.³³

From the obtained results, we can find that the complexes could be activated by VC, but such activation was dependent on the coordination structure of Pt(IV) complexes and slower than NQO1-triggered activation. Taken together, the measurements had revealed that our designed complexes could be effectively activated by both NQO1 and VC, thus showing a dual stimuli-responsive property as desired.

Fluorescence Spectroscopy and Confocal Microscopy. Complex 3 contained a fluorescent coumarin moiety (11) which may allow to visualize the action behavior of 3 in vitro. Thus, for the investigation of the optical properties, the fluorescence spectra of 11 and 3 were then monitored, respectively (Figure 3A). When the complexes were excited at the wavelength of 320 nm, 3 ($\Phi = 0.12$) showed an emission band at 397 nm. However, its fluorescence intensity was much weaker than that of 11 ($\Phi = 0.32$). Since 3 has been proved to be able to release 11 after the activation of NQO1 or VC, the fluorescence of 3 may be “turned on” in the presence of stimuli. In order to confirm this assumption, the fluorescence response of 3 in A549 (NQO1+) and LO2 (NQO1–) cells was investigated by laser scanning confocal microscopy. The results are shown in Figures 3B and S10. It was found that only weak fluorescence was observed in LO2 cells. In contrast, when 3 was incubated with A549 cells, strong fluorescence was observed at the nucleus site. In the case of 11, faint fluorescence was observed in both LO2 and A549 cells. Consequently, 3 could significantly accumulate in the NQO1 positive A549 cells in which it was specifically activated by

NQO1 to turn on the fluorescence. Thus, complex 3 might be considered as a targeting visual agent.

Comet Assay and Cell Cycle Analysis. It is well accepted that the antitumor activity of Pt(IV) complexes depends on the release of the corresponding Pt(II) species which then damage the target DNA. Since we have proven that our Pt(IV) complexes could release Pt(II) species upon the stimuli, the ability of complexes 1–3 to damage DNA was examined by comet assay.¹⁷ In this assay, the length of tail DNA has a positive correlation with the genotoxicity. As shown in Figures 4A, positive control cisplatin (5 μ M) caused moderate damage to DNA. In contrast, complexes 1–3 caused a much longer length of DNA tails, indicating their stronger DNA-damaging abilities than cisplatin. For deeper insight on the mode of action, we further assayed the effect of these complexes on cell cycle progression (Figure 4B). In A549 cells, cisplatin arrested the cell cycle mainly at the G2 phase (18.5% compared with 9.2% in the control). In contrast, the fraction of G2 phase increased to 16.3%, 23.9%, and 17.3% when cells were treated with 1, 2, and 3, respectively. Notably, the treatment of 2 or 3 significantly caused the increase of the percentage of sub-G1 phase, indicating a high level of DNA damage and apoptosis. Furthermore, the Pt(IV) complexes could also arrest the cell cycle at S phase (34.41% for 1, 35.16% for 2, and 37.88% for 3), demonstrating that the introduction of 6 to Pt(IV) complexes brought in a different action mode to kill cancer cells from cisplatin.

Cellular Uptake. It is well-known that the amount of cellular uptake of the Pt complexes has a great influence on the cytotoxicity. In fact, increased drug efflux is one of main mechanisms of cisplatin resistance.³⁴ Since the structural modifications may significantly change the lipophilicity of the complexes, Pt accumulation of 1–3 and cisplatin in A549 and A549/CDDP cells were measured by inductively coupled plasma mass spectrometry (ICP-MS) (Figure 5). The uptake

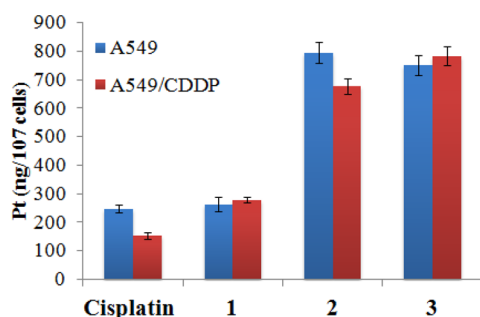


Figure 5. Cell uptake of cisplatin and complexes 1–3 in A549 and A549/CDDP cells.

of complex 1 in A549 cells was close to that of cisplatin, while the levels of 2 and 3 were significantly higher than that of cisplatin. The data were in accordance with the 3-(4,5-dimethyl-2-thiazolyl)-2,5-diphenyl-2H-tetrazolium bromide (MTT) results, suggesting that the Pt accumulation was largely responsible for the cytotoxicity of prodrugs 1–3. When A549/CDDP cells were employed, the uptake of cisplatin significantly decreased as expected. In contrast, the cellular uptake of 2 and 3 did not show an apparent decrease as compared with that of A549 cells. Given the higher cytotoxicity of 2 and 3 against A549/CDDP cells, this finding suggested that the high cellular uptake may, at least partly, be responsible for the ability of 2 and 3 to overcome the cisplatin-resistance.

Western Blot Analysis. For further exploration of the molecular mechanisms, Western blot analysis on complexes 1–3 was carried out in A549 cells (Figure 6). The expression of

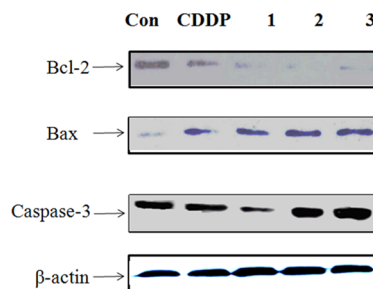


Figure 6. Western blot analysis of the expression of related proteins with cisplatin and complexes 1–3.

Bax, Bcl-2, and caspase-3 were determined by Western blotting with β -actin used as a loading control. The results turned out that the co-treatment with 1, 2, or 3 could significantly increase the expression of Bax while suppress the expression of Bcl-2. As far as the Bax and Bcl-2 were concerned, 2 and 3 showed stronger inhibitory effects than cisplatin and 1, confirming the assumption that apoptosis was conspicuously promoted.

In Vivo Antitumor Activity. In vivo antitumor efficacy of 2 and 3 on A549 tumor xenograft mice models was analyzed together with cisplatin. The tumor volumes were measured every 3 days for 28 days (Figure 7A). In the group of cisplatin, a moderate tumor inhibition was achieved in comparison with the vehicle group. Both treatments of 2 and 3 led to significant dose-dependent inhibition of the tumor growth. Tumor weight was also measured to clearly show the antitumor activity at the end of treatments. Accordingly, the tumor inhibition rates (IR) were 51.54, 54.95, 63.14, 30.72, and 66.89% for cisplatin (5.0 mg/kg), 2 (5.0 mg/kg), 2 (9.4 mg/kg), 3 (5.0 mg/kg), and 3 (12.7 mg/kg), respectively. Complex 2 exhibited a higher antitumor efficiency than cisplatin both at the equal mass dosage and the equimolar dosage, while 3 displayed the best antitumor activity at the equimolar dosage. No apparent body weight decrease was observed for mice treated with 2 and 3 (Figure 7B), suggesting the low systemic toxicity of these Pt(IV) prodrugs.

CONCLUSION

In summary, we have designed and synthesized three NQO1-targeting Pt(IV) hybrids containing a quinone propionic acid unit. These novel Pt(IV) complexes are stable under normal physiological conditions, but can be specifically activated by either NQO1 or VC which was overexpressed in numerous cancer cells. Confocal microscopy study revealed complex 3 with a coumarin moiety could selectively accumulate in NQO1+ A549 cells and subsequently be activated by NQO1 to switch on the fluorescence, thus 3 may act as an imaging and therapy agent. In MTT assay, 2 and 3 exhibited much better anticancer activities than cisplatin toward the NQO1 positive tumor cells. More importantly, they also significantly overcame cisplatin resistance. This may be attributed to the NQO1 targeting ability, improved cellular uptake, or different action mechanism. It was found that the Pt(IV) complexes could cause the DNA damage, arrest cell cycle, and induce apoptosis in A549 cells. Western blotting study showed that the complexes could up-regulate the expression level of caspase-3

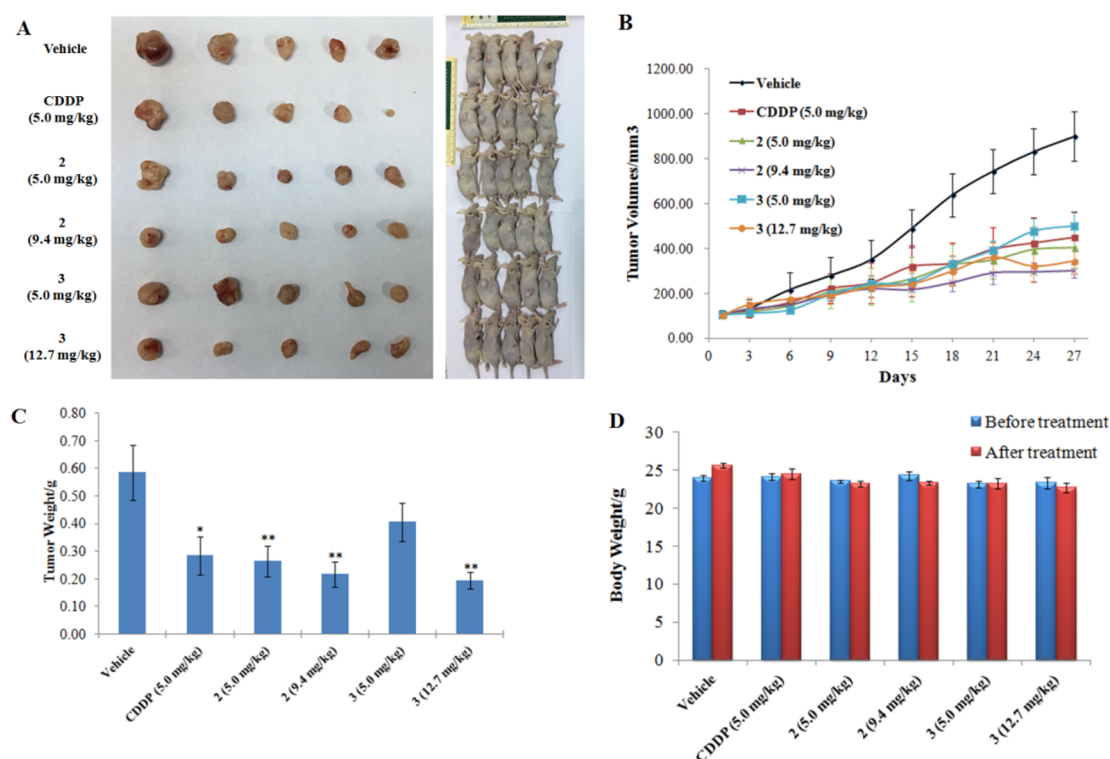


Figure 7. In vivo antitumor activity of compounds in mice bearing A549 xenograft. (A) The images of tumors at the end of the experiments. (B) Changes of tumor volumes after intravenous injection. (C) The tumor weight in each group at the end of the experiments. (D) Body weight of the mice from each group before and after the treatments. The data are presented as the mean \pm SEM * P < 0.05, ** P < 0.01, compared with control group.

and Bax and induce the proteolytic cleavage of Parp. In vivo study revealed that complexes **2** and **3** both exhibited higher antitumor efficacy than cisplatin in the A549 xenograft mouse model at the equimolar dose to cisplatin. In conclusion, this work has provided a dual stimuli-responsive Pt(IV) prodrug (complex **3**) which could targetingly act on the NQO1 positive tumor cells, overcome cisplatin resistance, and visualize the in vitro behavior.

EXPERIMENTAL SECTION

Materials and Instruments. All analytical grade chemicals and solvents were obtained from commercial purchase and used without further purification, unless noted specifically. The starting complexes c,c,t -[Pt(NH₃)₂Cl₃(OH)] and c,c,t -[Pt(NH₃)₂Cl₂(OH)₂] were self-prepared according to literature reports.¹ All antibodies used in this work were obtained from Santa Cruz Biotechnology. The cancer and normal cell lines were supplied by Jiangsu KeyGEN BioTECH company (China). Fluorescence spectra were recorded using a Fluoromax-4 spectrofluorometer (HORIBA) equipped with a xenon lamp. Cell cycle and apoptosis experiments were measured by flow cytometry (FAC Scan, Becton Dickinson) and analyzed by Cell Quest software. ¹H- and ¹³C NMR spectra were recorded in dimethylsulfoxide (DMSO)-*d*₆ on a Bruker 300 MHz spectrometer. ¹⁹⁵Pt-NMR spectra were measured in DMSO-*d*₆ on a Bruker 600 MHz spectrometer. Platinum contents were measured by ICP-MS (Optima 5300DV, PerkinElmer, USA). Mass spectrometry were measured by an Agilent 6224 ESI/TOF MS instrument. Elemental analyses for C, H, and N were done on a Vario MICRO CHNOS elemental analyzer (Elementar).

Synthesis. Preparation of 5. Compound **5** was prepared in 75% yield using a previously reported procedure.²⁷ ¹H NMR (300 MHz, CDCl₃): δ 1.46 (6H, s), 2.18 (3H, s), 2.22 (3H, s), 2.36 (3H, s), 2.55 (2H, s).

Preparation of 6. Compound **6** was prepared in 94% yield using a previously reported procedure.²⁷ ¹H NMR (300 MHz, DMSO-*d*₆): δ 1.33 (6H, s), 1.85 (3H, s), 1.86 (3H, s), 2.03 (3H, s), 2.81 (2H, s).

Preparation of 11. Compound **11** was prepared in 89% yield using a previously reported procedure.³⁵ ¹H NMR (300 MHz, DMSO-*d*₆): δ 4.82 (s, 2H), 6.82–6.32 (d, 1H, J = 9.5 Hz), 6.94–6.97 (m, 2H), 7.62–7.65 (d, 1H, J = 9.2 Hz), 7.97–8.00 (d, 1H, J = 9.5 Hz), 13.09 (s, 1H).

Preparation of 1. For the synthesis of **1**, a previously reported method was used.³⁵ Generally, TBTU (105.6 mg, 0.33 mmol) and **6** (82.6 mg, 0.33 mmol) were dissolved in 10 mL of anhydrous *N,N'*-dimethylformamide (DMF), and the resulted solution was stirred at room temperature in N₂ atmosphere for 10 min. Thereafter, triethylamine (TEA) (33.3 mg, 0.33 mmol) was added, and the obtained solution was stirred for 15 min. After the addition of c,c,t -[Pt(NH₃)₂Cl₃(OH)] (115.8 mg, 0.33 mmol), the reaction mixture was stirred at room temperature for 12 h. The solvent was then removed under reduced pressure, and the obtained residue was further purified by column chromatography (eluent 15:1 dichloromethane (DCM)/Methanol) to give **1** as a yellow solid (87.2 mg, 45.3%). ESI-HRMS: calcd for m/z [M – H][–] 583.0276, found 583.0298. ¹H NMR (300 MHz, DMSO-*d*₆): δ 1.36 (s, 6H), 1.86 (s, 3H), 1.92 (s, 3H), 2.05 (s, 3H), 2.81 (s, 2H), 5.98–6.23 (m, 6H). ¹³C NMR (75 MHz, DMSO-*d*₆): δ 12.38, 13.23, 14.35, 29.11, 38.91, 50.35, 137.61, 137.67, 143.40, 153.62, 180.24, 187.43, 190.73. ¹⁹⁵Pt-NMR (129 MHz, DMSO-*d*₆): δ 554 ppm. Anal. calcd for C₁₄H₂₃Cl₃N₂O₄Pt: C 28.75, H 3.96, N 4.79%. Found: C 28.53, H 4.09, N 4.55%.

Preparation of 2. Complex **2** was prepared in 23% yield using the same method of complex **1**. ESI-HRMS: calcd for m/z [M – H][–] 565.0621, found 565.0477. ¹H NMR (300 MHz, DMSO-*d*₆): δ 1.36 (s, 6H), 1.86 (s, 3H), 1.92 (s, 3H), 2.05 (s, 3H), 2.81 (s, 2H), 5.98–6.23 (m, 6H). ¹³C NMR (75 MHz, DMSO-*d*₆): δ 12.38, 13.23, 14.35, 29.11, 38.91, 50.35, 137.61, 137.67, 143.40, 153.62, 180.24, 187.43, 190.73. ¹⁹⁵Pt-NMR (129 MHz, DMSO-*d*₆): δ 1058 ppm. Anal. calcd

for $C_{14}H_{24}Cl_2N_2O_5Pt$: C 29.69, H 4.27, N 4.95%. Found: C 29.43, H 4.36, N 4.70%.

Preparation of 3. Complex 3 was prepared in 49% yield using the same method of complex 1. ESI-HRMS: calcd for m/z $[M - H]^-$ 767.0892, found 767.0916. 1H NMR (300 MHz, DMSO- d_6): δ 1.34 (s, 6H), 1.88 (s, 3H), 1.92 (s, 3H), 2.05 (s, 3H), 2.84 (s, 2H), 4.73 (s, 2H), 6.26–6.29 (d, 2H, $J = 10.0$ Hz), 6.46 (m, 6H), 6.91–6.94 (dd, 1H, $J = 2.3, 8.7$ Hz), 6.98 (d, 1H, $J = 2.0$ Hz), 7.57–7.60 (d, 1H, $J = 8.6$ Hz), 7.96–7.99 (d, 1H, $J = 9.6$ Hz). ^{13}C NMR (75 MHz, DMSO- d_6): δ 12.32, 13.17, 14.31, 28.98, 38.73, 40.00, 49.53, 65.22, 102.12, 112.97, 113.35, 113.42, 129.68, 137.59, 137.66, 143.43, 144.72, 153.50, 155.67, 160.74, 161.72, 175.34, 180.25, 187.39, 190.68. ^{195}Pt -NMR (129 MHz, DMSO- d_6): δ 1260 ppm. Anal. calcd for $C_{25}H_{30}Cl_2N_2O_9Pt$: C 39.07, H 3.93, N 3.65%. Found: C 38.75, H 3.99, N 3.48%.

UV-vis Experiments. Complexes 1–3 were dissolved in PBS under different pH values, and the final concentration was set to 0.1 mM. Then the UV absorption of the samples was recorded on a Shimadzu UV2600 instrument equipped with a thermostatically controlled cell holder with wavelength ranging from 190 to 450 nm. All the experiments were carried out at 37 ± 0.1 °C.

Stability of 1–3 in Medium RPMI-1640 Containing 10% Fetal Bovine Serum. A HPLC study was performed to investigate the stability of Pt(IV) complexes in RPMI-1640 (containing 10% fetal bovine serum (FBS)). Complexes 1–3 were dissolved in PBS with 5% DMF, and the concentration was set to 20 mM. The complexes were added into RPMI-1640 and incubated for 0, 6, 12, 18, and 24 h at 37 °C, respectively. Reversed phase HPLC was implemented on a 250×4.5 mm ODS column. The chromatograms were recorded on UV detection at 210 nm. The flow rate used for the study was set to 1.0 mL/min. Before the HPLC analysis, the samples were filtrated by 0.45 μ m filter. For the calculation of the relative ratio, the HPLC peak at 0 h was used as the reference (i.e., 100%), then the HPLC peak at a different time point was compared with the reference peak to calculate the relative ratio.

Cyclic Voltammetry. The CV was carried out on PGSTAT101 (Autolab, Metrohm) with a three-electrode setup comprising a glassy carbon working electrode, platinum wire auxiliary electrode, and a calomel reference electrode. The scan started from -1.0 V to $+1.0$ V. The tested sample was prepared by dissolving the complex in PBS containing 5% DMF, and the final concentration was 20 mM. The scan rate was 100 mV \cdot s $^{-1}$ at 25 °C. KCl solution (0.1 M, pH 7.0) was used as a background electrolyte.

Preparation of Stock Solutions for Cellular Studies. The stock solution was prepared by dissolving the organic compounds or the platinum(IV) complex in DMF to a final concentration of 20 mM. The stock solution was serially diluted before the test. The final DMF concentration in culture medium was <0.4%. For cisplatin, the stock solution was prepared by dissolving cisplatin in water and was diluted directly into culture medium when used.

Cell Culture. All adherent cell lines including HepG-2 (human hepatocellular carcinoma cell line), A549 (human lung carcinoma cell line), LO2 (human hepatic cell line), and A549/CDDP (human lung carcinoma cell line-cisplatin resistance) were cultured in a humidified, 5% CO₂ atmosphere at 37 °C and maintained in monolayer culture in RPMI-1640 medium supplemented with 10% FBS, 100 μ g/mL of penicillin and 100 μ g/mL of streptomycin.

Cytotoxicity Measurement. The cell viability was determined by 3-(4,5-dimethylthiazol-2-yl)-2,5-diphenyltetrazolium bromide (MTT) assay. The tested compounds were dissolved in DMF and diluted to the required concentration with culture medium (DMF final concentration <0.4%). The suspension of 5000 cells/well was plated in 96-well culture plates with culture medium and was incubated overnight at 37 °C, in a 5% CO₂ incubator. Then the tested compound solution was added. Cells were incubated at 37 °C for 72 h, respectively. After that, the cells were treated with 10 mL MTT dye solution (5 mg/mL) for 4 h cultivation. After the media with MTT solution were removed with 100 mL of DMSO solution, the absorbance of formazane solution was measured with an ELISA reader at 570 nm. Wells without cells were used as blanks and were

subtracted as background from each sample. The IC₅₀ values were calculated by SPSS software after three parallel experiments, and the results were expressed as the mean \pm SD.

Stimuli-Responsive Property of 1–3 Treated with NQO1 or VC. The activation of Pt(IV) complexes was determined by HPLC using VC or NQO1 as the stimuli. The final concentration of NQO1 was set to 100 μ g/mL and 1 mM for VC. Complexes 1–3 were used at the concentration of 0.1 mM. Reversed phase HPLC was implemented on a 250×4.5 mm ODS column. The chromatograms were recorded on UV detection at 210 nm. The flow rate used for the study was set to 1.0 mL/min. Before the HPLC analysis, the samples were filtrated by 0.45 μ m filter.

Confocal Microscopy. Confocal microscopy was performed to investigate the cellular localization of tested compounds (5 μ M) in A549 and LO2 cells. Generally, 0.5×10^6 cells were seeded on the 35 mm glass bottom dishes (MatTek). Then the tested compounds were added, and the cells were co-incubated at 37 °C under 5% CO₂ for 3 h. Then 15 min before the end of the co-incubation, DAPI was added for nucleus staining. After washed three times with PBS, the cells were further incubated in colorless serum-free media for 15 min and then imaged by a confocal laser scanning microscope (Zeiss LSM 700, Zeiss, Germany. Ex: 335 nm; Em: 490–520 nm). Fluorescence from DAPI appears as blue signals (Ex: 340 nm; Em: 450–470 nm).

Determination of Quantum Yields. In this study, Rhodamine B ($\Phi = 0.59$) was used as a standard, and the test was performed at 25 °C. The absorption of Rhodamine B was adjusted to the same value (abs <0.1) as that of fluorescent molecules. Excitation wavelength was set at 320 nm, and the emission spectra were recorded in the range from 340 to 520 nm. The quantum yields were calculated by the equation: $\Phi_{\text{sample}} = \Phi_{\text{standard}} (F_{\text{sample}}/F_{\text{standard}}) (A_{\text{standard}}/A_{\text{sample}})$, where Φ is the quantum yield, F is the integration of emission intensity, and A is the absorbance value at excitation wavelength.

Cellular Uptake Test. A549 and A549/CDDP cells were seeded in 6-well plates at 37 °C under 5% CO₂, respectively. After the cell density reached 80%, cisplatin or complexes 1–3 (final concentration 5 μ M) was added and then co-incubated for further 24 h. After that, cells were collected, washed three times with ice-cold PBS, centrifuged for 10 min, and resuspended in PBS. The obtained suspension (100 μ L) was used for determining the cell density. HNO₃ (200 μ L, 65%) was used to digest the remaining cells. Finally, ICP-MS was employed to quantify the results via three parallel experiments.

Comet Assay. A549 cells (1×10^5) and cisplatin or complexes 1–3 were co-incubated for 24 h, respectively, and then molten LM Agarose (Trevigen) at a ratio of 1/10 (v/v) was added. Thereafter, the mixture was quickly transferred onto Comet Slide (Trevigen). The samples were incubated at 4 °C for another 10 min in the dark and then immersed in Lysis buffer and stood at 4 °C for 0.5 h. Slides were then treated with alkaline unwinding solution prepared by mixing 1 mM EDTA and 200 mM NaOH for 20 min at 25 °C in the dark. For the electrophoresis, alkaline electrophoresis solution (1 mM EDTA, 200 mM NaOH) was used at 21 V for 0.5 h. The slides were immersed in water twice for 5 min and then washed once by 70% EtOH. After drying overnight, the slides were visualized by microscopy.

Cell Cycle Measurement. A549 cells (10 000 per well) were cultured in 6-well plates overnight at 37 °C. Then, 5 μ M of the tested compounds were added and co-incubated with cells for 24 h. All cells, including adherent and floating cells, were collected and washed twice with PBS and then fixed by 70% EtOH at 4 °C for 24 h. After that, fixed cells were washed with PBS. Thereafter, the cells were centrifuged, stained with 50 μ g/mL propidium iodide (PI) solution containing 100 μ g/mL RNase at 37 °C for 0.5 h. Finally, the sample was measured by flow cytometry using Cell Quest software and recording PI in the FL2 channel.

Western Blot Analysis. The A549 cells and 5 μ M of the compounds were co-incubated for 24 h at 37 °C. Then the proteins were extracted, and the concentration of protein was measured by the bicinchoninic acid (BCA) assay with a Varioskan multimode microplate spectrophotometer (Thermo, Waltham, MA). After the

separation of the proteins (20 mg/Lane) by 10% sodium dodecyl sulfate-polyacrylamide gel electrophoresis (SDS-PAGE), protein samples were transferred onto polyvinylidene difluoride (PVDF) Immobilon-P membrane (Bio-Rad). The blots were first blocked with 5% nonfat milk in TBST for 1 h and then co-incubated with primary antibodies which were diluted in PBST overnight at 4 °C. After washed with PBST for three times, the membrane was incubated with IRDye 800 conjugated secondary antibody for 1 h at 37 °C. Finally the results were obtained by an Odyssey scanning system (Li-COR, Lincoln, Nebraska).

In Vivo Studies. The in vivo antitumor activity was determined using A549 cell line in BALB/c nude mice. Six-week-old BALB/c nude mice (18–22 g) were obtained from Shanghai Ling Chang biotechnology company (China); tumors were formed by subcutaneously injecting 10^7 cells in 100 μ L sterile PBS into the dorsal region of mice. When the tumor volume reached 100–150 mm³, the mice were randomly divided into 6 groups with 5 mice in each group: (1) cisplatin (5.0 mg/kg) treated group; (2) **2** (5.0 mg/kg) treated group; (3) **2** (9.4 mg/kg, equimolar to the cisplatin group) treated group; (4) **3** (5.0 mg/kg) treated group; (5) **3** (12.7 mg/kg, equimolar to the cisplatin group) treated group; and (6) vehicle group (5% dextrose injection). The mice were administered intravenously with the above-mentioned formulations once a week for a period of 28 days. Tumor volume and body weight were measured every other day after drug administration. After 4 weeks of treatment, all of the mice were sacrificed, and tumor volumes were determined by measuring length (A) and width (B) of the tumor to calculate volume ($V = AB^2/2$).

■ ASSOCIATED CONTENT

● Supporting Information

The Supporting Information is available free of charge on the ACS Publications website at DOI: 10.1021/acs.inorgchem.8b03386.

Diagrams of ESI-MS, ¹H-, ¹³C-, and ¹⁹⁵Pt-NMR spectra. Cyclic voltammograms of complexes **1**–**3**. HPLC analyses on the purity as well as the stability and the released ability of Pt(IV) complexes under reduction with VC or NQO1. Confocal microscopy images (PDF)

■ AUTHOR INFORMATION

Corresponding Author

*E-mail: sgou@seu.edu.cn.

ORCID

Shaohua Gou: 0000-0003-0284-5480

Notes

The authors declare no competing financial interest.

■ ACKNOWLEDGMENTS

We are grateful to the National Natural Science Foundation of China (grant no. 21571033) for financial aids to this work. Jiangsu KeyGen Biotech Company is appreciated for completing the in vivo antitumor activity test. We thank Prof. Hengshan Wang (School of Chemistry and Pharmaceutical Sciences, Guangxi Normal University) for a license to use their molecular docking software. X.Q. is grateful to the Innovation Program of Jiangsu Province Postgraduate Education (Project KYLX15_0128). L.F. thanks the State Key Laboratory for Chemistry and Molecular Engineering of Medicinal Resources (Guangxi Normal University) (CMEMR2017-B05) for financial support. The authors would also like to thank the Fundamental Research Funds for the Central Universities (Project 2242016k30020) for supplying basic facilities to our key laboratory. We also want to express our gratitude to the Priority Academic Program

Development of Jiangsu Higher Education Institutions for the construction of fundamental facilities.

■ REFERENCES

- (1) Torre, L. A.; Bray, F.; Siegel, R. L.; Ferlay, J.; Lortet-Tieulent, J.; Jemal, A. Global cancer statistics, 2012. *Ca-Cancer J. Clin.* **2015**, *65*, 87–108.
- (2) Ismael, G. F.; Rosa, D. D.; Mano, M. S.; Awada, A. Novel cytotoxic drugs: old challenges, new solutions. *Cancer Treat. Rev.* **2008**, *34*, 81–91.
- (3) Holohan, C.; Van Schaeybroeck, S.; Longley, D. B.; Johnston, P. G. Cancer drug resistance: an evolving paradigm. *Nat. Rev. Cancer* **2013**, *13*, 714–726.
- (4) Srinivasarao, M.; Galliford, C. V.; Low, P. S. Principles in the design of ligand-targeted cancer therapeutics and imaging agents. *Nat. Rev. Drug Discovery* **2015**, *14*, 203–219.
- (5) Ren, W. X.; Han, J.; Uhm, S.; Jang, Y.; Kang, C.; Kim, J. H.; Kim, J. S. Recent development of biotin conjugation in biological imaging, sensing, and target delivery. *Chem. Commun.* **2015**, *51*, 10403–10418.
- (6) Weinstein, R.; Segal, E.; Satchi-Fainaro, R.; Shabat, D. Real-time monitoring of drug release. *Chem. Commun.* **2010**, *46*, 553–555.
- (7) Wu, X. M.; Sun, X. R.; Guo, Z. Q.; Tang, J. B.; Shen, Y. Q.; James, T. D.; Tian, H.; Zhu, W. H. In vivo and in situ tracking cancer chemotherapy by highly photostable NIR fluorescent theranostic prodrug. *J. Am. Chem. Soc.* **2014**, *136*, 3579–3588.
- (8) Bhuniya, S.; Maiti, S.; Kim, E. J.; Lee, H.; Sessler, J. L.; Hong, K. S.; Kim, J. S. An activatable theranostic for targeted cancer therapy and imaging. *Angew. Chem., Int. Ed.* **2014**, *53*, 4469–4474.
- (9) Li, S. Y.; Liu, L. H.; Jia, H. Z.; Qiu, W. X.; Rong, L.; Cheng, H.; Zhang, X. Z. A pH-responsive prodrug for real-time drug release monitoring and targeted cancer therapy. *Chem. Commun.* **2014**, *50*, 11852–11855.
- (10) Dinkova-Kostova, A. T.; Talalay, P. NAD(P)H: quinone acceptor oxidoreductase 1 (NQO1), a multifunctional antioxidant enzyme and exceptionally versatile cytoprotector. *Arch. Biochem. Biophys.* **2010**, *501*, 116–123.
- (11) Danson, S.; Ward, T. H.; Butler, J.; Ranson, M. DT-diaphorase: a target for new anticancer drugs. *Cancer Treat. Rev.* **2004**, *30*, 437–449.
- (12) Tong, Y. H.; Zhang, B.; Yan, Y. Y.; Fan, Y.; Yu, J. W.; Kong, S. S.; Zhang, D.; Fang, L.; Su, D.; Lin, N. M. Dual-negative expression of Nrf2 and NQO1 predicts superior outcomes in patients with non-small cell lung cancer. *Oncotarget.* **2017**, *8*, 45750–45758.
- (13) Oh, E. T.; Park, H. J. Implications of NQO1 in cancer therapy. *BMB Rep.* **2015**, *48*, 609–617.
- (14) Ma, X.; Moore, Z. R.; Huang, G.; Huang, X.; Boothman, D. A.; Gao, J. Nanotechnology-enabled delivery of NQO1 bioactivatable drugs. *J. Drug Target.* **2015**, *23*, 672–680.
- (15) Silvers, W. C.; Prasai, B.; Burk, D. H.; Brown, M. L.; McCarley, R. L. Profluorogenic reductase substrate for rapid, selective, and sensitive visualization and detection of human cancer cells that overexpress NQO1. *J. Am. Chem. Soc.* **2013**, *135*, 309–314.
- (16) Hsu, D. S.; Balakumaran, B. S.; Acharya, C. R.; Vlahovic, V.; Walters, K. S.; Garman, K.; Anders, C.; Riedel, R. F.; Lancaster, J.; Harpole, D.; et al. Pharmacogenomic strategies provide a rational approach to the treatment of cisplatin-resistant patients with advanced cancer. *J. Clin. Oncol.* **2007**, *25*, 4350–4357.
- (17) Rabik, C. A.; Dolan, M. E. Molecular mechanisms of resistance and toxicity associated with platinating agents. *Cancer Treat. Rev.* **2007**, *33*, 9–23.
- (18) Wang, Z. G.; Xu, Z. F.; Zhu, G. Y. A platinum(IV) anticancer prodrug targeting nucleotide excision repair to overcome cisplatin resistance. *Angew. Chem., Int. Ed.* **2016**, *55*, 15564–15568.
- (19) Chen, F. H.; Huang, X. C.; Wu, M.; Gou, S. H.; Hu, W. W. A CK2-targeted Pt(IV) prodrug to disrupt DNA damage response. *Cancer Lett.* **2017**, *385*, 168–178.
- (20) Pathak, R. K.; Marrache, S.; Choi, J. H.; Berding, T. B.; Dhar, S. The Prodrug Platin-A: Simultaneous Release of Cisplatin and Aspirin. *Angew. Chem., Int. Ed.* **2014**, *53*, 1963–1967.

(21) Cheng, Q.; Shi, H.; Wang, H.; Min, Y.; Wang, J.; Liu, Y. The ligation of aspirin to cisplatin demonstrates significant synergistic effects on tumor cells. *Chem. Commun.* **2014**, *50*, 7427–7430.

(22) Shi, Y.; Liu, S. A.; Kerwood, D. J.; Goodisman, J.; Dabrowiak, J. C. Pt(IV) complexes as prodrugs for cisplatin. *J. Inorg. Biochem.* **2012**, *107*, 6–14.

(23) Ma, L.; Ma, R.; Wang, Y.; Zhu, X.; Zhang, J.; Chan, H. C.; Chen, X.; Zhang, W.; Chiu, S. K.; Zhu, G. Chalcoplatin, a dual-targeting and p53 activator-containing anticancer platinum(IV) prodrug with unique mode of action. *Chem. Commun.* **2015**, *51*, 6301–6304.

(24) Hall, M. D.; Hambley, T. W. Platinum(IV) antitumour compounds: their bioinorganic chemistry. *Coord. Chem. Rev.* **2002**, *232*, 49–67.

(25) Johnstone, T. C.; Suntharalingam, K.; Lippard, S. The next generation of platinum drugs: targeted Pt(II) agents, nanoparticle delivery, and Pt(IV) prodrugs. *Chem. Rev.* **2016**, *116*, 3436–3486.

(26) Wexselblatt, E.; Gibson, D. What do we know about the reduction of Pt(IV) pro-drugs? *J. Inorg. Biochem.* **2012**, *117*, 220–229.

(27) Carpino, L. A.; Triolo, S. A.; Berglund, R. A. Reductive lactonization of strategically methylated quinone propionic acid esters and amides. *J. Org. Chem.* **1989**, *54*, 3303–3310.

(28) Ravera, M.; Gabano, E.; Pelosi, G.; Fregonese, F.; Tinello, S.; Osella, D. A new entry to asymmetric platinum(IV) complexes via oxidative chlorination. *Inorg. Chem.* **2014**, *53*, 9326–9335.

(29) Bouché, M.; Bonnefont, A.; Achard, T.; Bellemin-Lapponnaz, S. Exploring diversity in platinum(IV) N-heterocyclic carbene complexes: synthesis, characterization, reactivity and biological evaluation. *Dalton Trans.* **2018**, *47*, 11491–11502.

(30) Ong, W.; Yang, Y.; Cruciano, A. C.; McCarley, R. L. Redox-triggered contents release from liposomes. *J. Am. Chem. Soc.* **2008**, *130*, 14739–14744.

(31) Shin, W. S.; Lee, M. G.; Verwilt, P.; Lee, J. H.; Chi, S. G.; Kim, J. S. Mitochondria-targeted aggregation induced emission theranostics: crucial importance of in situ activation. *Chem. Sci.* **2016**, *7*, 6050–6059.

(32) Lemma, K.; House, D. A.; Retta, N.; Elding, L. I. *Inorg. Chim. Acta* **2002**, *331*, 98–108.

(33) Zhang, J. Z.; Wexselblatt, E.; Hambley, T. W.; Gibson, D. Pt(IV) analogs of oxaliplatin that do not follow the expected correlation between electrochemical reduction potential and rate of reduction by ascorbate. *Chem. Commun.* **2012**, *48*, 847–849.

(34) Borst, P.; Kool, M.; Evers, R. Do cMOAT (MRP2), other MRP homologues, and LRP play a role in MDR. *Semin. Cancer Biol.* **1997**, *8*, 205–213.

(35) Qin, X.; Fang, L.; Zhao, J.; Gou, S. Theranostic Pt(IV) conjugate with target selectivity for androgen receptor. *Inorg. Chem.* **2018**, *57*, 5019–5029.